DE-13-001

General Correlation For Heat Transfer During Condensation in Plain Tubes: Further Development and Verification

Mirza Mohammed Shah, PhD, PE
Fellow ASHRAE

ABSTRACT

Further development and verification of the author's general correlation is presented. While this correlation is also applicable to vertical tubes, only horizontal tubes are addressed in this paper. The boundary between the mixed and laminar heat transfer regimes for horizontal tubes was hitherto undefined. An equation to determine this boundary is presented. The relation between these heat transfer regimes and flow pattern regimes is investigated. The correlation is compared to additional data for horizontal tubes, which include very low flow rates and fluids not included in the earlier paper. A total of 547 data points from 11 studies are analyzed. The data include CO_2 near critical pressure as well as seven other fluids. Together with the previously analyzed data for all orientations, this correlation has been verified with 1736 data points from 51 studies that include 24 fluids.

INTRODUCTION

Over three decades ago, the author had presented a general correlation for heat transfer during film condensation inside plain tubes (Shah 1979). While this correlation found wide acceptance, it is limited to higher flow rates and moderate pressures. The author presented an improved version that extended its applicability to low flow rates and pressures near critical pressure. It was shown to be in good agreement with data for 22 fluids in horizontal, vertical, and inclined tubes over a very wide range of flow rates and pressures (Shah 2009). Its further development and verification for horizontal tubes is presented in this paper.

The 2009 correlation has three heat transfer regimes (turbulent, mixed, and laminar) called Regimes I, II, and III. Different formulas apply in each regime. While the boundaries between the three regimes were clearly demarcated for vertical tubes in the 2009 correlation, the boundary between Regimes II and III for horizontal tubes was not demarcated due to lack of sufficient data. This boundary was determined during the present research using newly published data.

The boundaries between the regimes have been determined exclusively on an empirical basis. It is of interest to see the relation between these heat transfer regimes and flow pattern regimes. This was done during the present research, as reported in this paper.

Presently, there is a great deal of interest in using carbon dioxide as a refrigerant as it does not deplete the ozone layer and has zero global warming potential (GWP). Comparison with carbon dioxide data was not included in the 2009 paper. Several studies for this fluid have recently been published and comparison with their data is presented here. Comparison with other recently published data was also done for further verification. These data include dimethyl ether (DME), a fluid not included in the verification data in the 2009 paper.

In Shah (2009), data analyzed included tubes of diameter 2 mm (0.079 in.) and larger. The present work has also been confined to diameters larger than 2 mm (0.079 in.). There are wide variations in published data for smaller channels and many views about the physical phenomena in them. The author has published a comparison of this correlation with such data (Shah 2010).

Mirza Mohammed Shah is a consultant in Redding, CT.

THE PUBLISHED SHAH CORRELATION 2009

Heat Transfer Equations

The correlation uses the following two heat transfer equations:

$$h_I = h_{LS}\left(1 + \frac{3.8}{Z^{0.95}}\right)\left(\frac{\mu_f}{14\mu_g}\right)^{(0.0058 + 0.557 p_r)} \quad (1)$$

The second equation is:

$$h_{Nu} = 1.32\mathrm{Re}_{LS}^{-1/3}\left[\frac{\rho_l(\rho_l - \rho_g)gk_f^3}{\mu_f^2}\right]^{1/3} \quad (2)$$

Equation 1 is the same as that in the Shah (1979) correlation except that the previous version did not have the viscosity ratio factor. Equation 2 is the Nusselt equation for laminar film condensation in vertical tubes; the constant has been increased by 20% as recommended by McAdams (1954) on the basis of comparison with test data. This equation can also be expressed in terms of heat flux or temperature difference instead of Reynolds number. This form has been preferred, as it is more convenient for this correlation and often it is also more convenient for design calculations.

These heat transfer equations are used as follows: For all tube orientations (except upward flow),

in Regime I,

$$h_{TP} = h_I \quad (3)$$

in Regime II,

$$h_{TP} = h_I + h_{Nu} \quad (4)$$

in Regime III,

$$h_{TP} = h_{Nu} \quad (5)$$

h_{LS} in Equation 1 is the heat transfer coefficient of the liquid phase flowing alone in the tube. It is calculated by the following equation:

$$h_{LS} = 0.023\mathrm{Re}_{LS}^{0.8}\mathrm{Pr}_f^{0.4}k_f/D \quad (6)$$

Heat Transfer Regimes for Horizontal Tubes

The boundary between Regimes I and II was determined through data analysis described in Shah (2009). The data that agreed with Equation 3 were considered to be in Regime I and those that agreed with Equation 4 were considered to be in Regime II. The data points were than plotted on a Z versus J_g graph. A curve was drawn through the boundary between the data for the two regimes and an equation fitted to it.According to this curve, Regime I occurs when

$$J_g \geq 0.98(Z + 0.263)^{-0.62} \quad (7)$$

Otherwise, it is Regime II. A third regime was expected at very low flow rates. Analyzable data were not available for such conditions. Hence, its boundary had to be left undefined. This boundary has been determined during the present research as described later.

In Equation 7, J_g is the dimensionless vapor velocity defined as:

$$J_g = \frac{xG}{(gD\rho_g(\rho_l - \rho_g))^{0.5}} \quad (8)$$

Z is the correlating parameter introduced by Shah (1979), defined as

$$Z = \left(\frac{1}{x} - 1\right)^{0.8} p_r^{0.4} \quad (9)$$

EFFORTS FOR FURTHER DEVELOPMENT

The Boundary Between Regimes II and III

By analyzing newly available data for low flow rates together with previously analyzed data, the boundary between Regimes II and III was determined as follows. Regime III occurs when:

$$J_g \leq 0.95(1.254 + 2.27Z^{1.249})^{-1} \quad (10)$$

Otherwise it is Regime I or II as determined by Equation 7. This boundary was determined by comparing the predictions of the correlation for Regimes II and III with the measured data. The data points were assigned to the regimes which gave better agreement with measurements. There was some scatter across this boundary but 85% of data agreed with it. Scatter indicates that while the boundary criterion indicates a data point to be in Regime II, the heat transfer coefficient is in agreement with the equation for Regime III or vice-versa; 15% of the data showed such scatter

Figure 1 shows the boundaries of the three heat transfer regimes. The curves have been limited to the range of data analyzed.

Relation with Flow Pattern Regimes

The heat transfer regimes defined in this correlation are purely empirical. Many predictive techniques for heat transfer and pressure drop, theoretical and empirical, are based on flow patterns. It was therefore investigated whether these heat transfer regimes can be defined on the basis of flow patterns. Many flow pattern maps are available. The flow pattern map of El Hajal et al. (2003) was shown by these authors to agree with a very wide range of data, including many fluids for condensation. It was therefore chosen. This correlation has five flow patterns, namely stratified, stratified wavy, intermittent, annular, and mist. Comparison of the predicted flow patterns with the predicted heat transfer regimes by Equations 7 and 10 gave the results shown in Table 1.

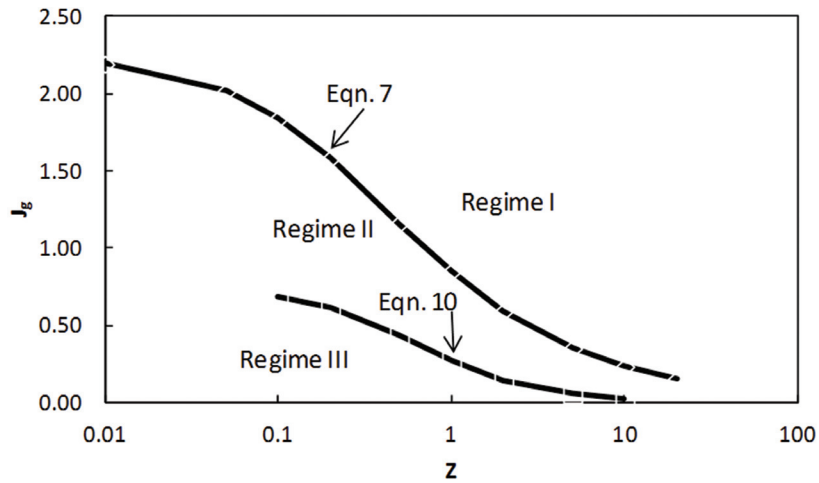

Figure 1 *Heat transfer regimes according to the present correlation.*

As seen in Table 1, the mist, annular, and intermittent regimes always correspond to Regime I, as predicted by the present correlation. However, the relationship with the stratified-wavy and stratified regimes is not so clear. While the majority of data in the stratified-wavy regime are in the predicted heat transfer Regime II, many others are in Regime III and a few are even in Regime I. The stratified regime includes data points in both Regimes II and III.

Thus, distinction between Regime II and III cannot be made using the El Hajal et al. map (2003). Many other flow pattern maps are available, for example Breber et al. (1980). It will be interesting to see whether any of them can be used to distinguish between Regimes II and III, but that study was outside the present scope.

COMPARISON WITH TEST DATA

A literature search was done to identify data published since the preparation of the Shah (2009) paper. Special emphasis was on finding data at low flow rates that may help developing the boundary between Regimes II and III. Special efforts were also made to locate data for carbon dioxide as its data were not analyzed in the 2009 paper and it is currently of great interest as a refrigerant. These efforts resulted in the collection of data whose range is given in Table 2.

The data collected were compared with the present correlation described in the foregoing. The single-phase heat transfer coefficient was calculated with Equation 6 for all data except for the data of Son and Lee (2009) for which the following equation was used:

$$h_{LS} = 0.034 \mathrm{Re}_{LS}^{0.8} \mathrm{Pr}_f^{0.3} k_f / D \tag{11}$$

The reason is that these authors' single-phase measurements were higher than Equation 7 and they fitted Equation 11 to their data.

All fluid properties were calculated at the saturation temperature using REFPROP 9.0 (Lemmon et al. 2010).

Table 1. Flow Patterns Predicted by the Correlation of El Hajal et al. (2003) Compared with the Heat Transfer Regimes According to the Present Correlation.

Predicted Flow Pattern	Predicted Heat Transfer Regime
Mist	I (always)
Annular	I (always)
Intermittent	I (always)
Stratified-wavy	70% II, 20% III, 10% I
Stratified	II or III

Results of Comparison of Data with the Present Correlation

The salient features of the new data that were analyzed are listed in Table 2.Some of the data were for mean heat transfer coefficients over the length of the tubes. Such data were analyzed by using the arithmetic average quality in calculations. It would be more correct to calculate local heat transfer coefficients along the length and then integrate them to get the predicted mean heat transfer coefficient, but it is not possible as distribution of quality along the length is not given in the papers. As discussed in Shah (1979), use of arithmetic mean quality gives a reasonable approximation to the more rigorous method.

Table 2 lists the average and mean deviations of the present correlation. Mean deviation δ_m is defined as:

$$\delta_m = \frac{1}{N}\sum_{N}^{1} ABS \frac{(h_{predicted} - h_{measured})}{h_{measured}} \tag{12}$$

Table 2. Range of Data Analyzed in the Present Work and Their Deviations with the Present Correlation.

Source	D mm (in.)	Fluid	p_r	G Kg/m^{2}s	G Lb/s.ft^2	x	Re_{LT}	Re_{GT}	Number of Data Points	Deviation Mean Average
Kondou and Hrnjak (2011)	6.1 (0.24)	CO_2	0.81	100 200	20.5 41.0	0.10 0.95	9687 19374	32472 64945	23	14.7 –12.1
			0.946	150	30.7	0.10 0.95	18729	40083	8	10.0 +0.4
Zilly et al. (2003)	6.1 (0.24)	CO_2	0.227 0.309	200 400	41.0 82.0	0.10 0.80	8046 18973	95529 191058	16	28.7 +28.7
Son and Oh (2012)	4.6 (0.18)	CO_2	0.774	400 800	82.0 164.0	0.10 0.88	27710 55419	101417 202834	26	23.9 +16.3
			0.869	800	164.0	0.11 0.90	64171	183285	9	36.7 +36.7
			0.931	800	164.0	0.10 0.90	72597	173062	9	106 +106
Iqbal and Bansal (2012)	6.52 (0.26)	CO_2	0.309 0.470	50 200	10.2 41.0	0.02 0.90	2535 13085	22071 94145	83	27.6 5.1
Zilly et al. (2003)	6.1 (0.24)	R-22	0.049 0.136	400	82.0	0.20 0.78	9031 12575	206932 231669	7	15.1 +14.1
Li and Ji-Tian (2007)	9.4 (0.37)	R-134a	0.249	100 400	20.5 82.0	0.10 0.80	5811 23245	76018 304071	20	6.4 –3.0
Wen et al. (2006)	2.46 (0.10)	Butane	0.1	205 510	42.0 104.5	0.12 0.84	3665 9118	64820 161260	18	15.1 –14.4
		R-134a	0.25	205 510	42.0 104.5	0.12 0.8	2551 6346	40072 99692	18	9.9 2.6
		Propane	0.32	205 510	42.0 510.0	0.12 0.80	6099 15174	53719 133642	18	10.8 –8.5
Afroz et al. (2008)	4.35 (0.17)	DME	0.13	200 500	41.0 102.5	.02 .94	7131 17828	92850 232124	29	12.2 –10.9
Son and Lee (2009)	3.36 (0.13) 5.35 (0.21)	R-22	0.308	300 400	61.5 82.0	0.08 0.88	4917 7830	70360 170048	18	12.3 –10.9
		R-134a	0.25	200 400	41.0 82.0	0.08 0.9	3399 10834	53398 106796	20	10.8 –7.5
		R-410A	0.49	200 400	41.0 82.0	0.05 0.92	7117 22663	45801 145855	28	9.6 –5.5
Lee and Son (2010)	5.8 (0.23) 6.54 (0.26) 7.73 (0.30) 10.07 (0.40)	Propane	0.32	47 170	9.6 34.8	0.05 0.85	3453 11882	32248 110976	46	15.5 –4.5
		Isobutane	0.146	49 170	10.0 34.8	0.05 0.87	2211 7609	36231 124681	47	20.1 –4.1
		R-22	0.306	50 155	10.2	0.06 0.89	6346 10873	66041 113152	46	23.0 +12.0
		R-134a	0.249	52 165	10.7 33.8	0.05 0.86	1510 7885	19747 103146	43	25.2 –28.0

Table 2. *(continued)* **Range of Data Analyzed in the Present Work and Their Deviations with the Present Correlation.**

Source	D mm (in.)	Fluid	p_r	G Kg/m²s	G Lb/s.ft²	x	Re_{LT}	Re_{GT}	Number of Data Points	Deviation Mean Average
Wilson et al. (2003)	3.7* (0.14)	R-134a	0.22	75 400	15.3 82.0	0.1 0.79	1386 7390	22701 121073	13	14.9 –3.9
		R-410A	0.44	75 400	15.3 82.0	0.1 0.8	2733 14577	19687 10499	12	15.8 15.5
		R-410A	0.44	75 400	15.3 82.0	0.1 0.8	2733 14577	19687 10499	12	15.8 15.5
Dalkilic and Agra (2009)	4.0 (0.16)	Isobutane	0.127	57 92	11.7 18.9	0.50 0.85	1671 2698	29362 47392	15	18.7 –18.7
All sources	2.46 (0.10) 10.07 (0.40)		0.127 0.946	47 800	9.6 164.0	0.02 0.95	1671 55419	22071 304071	547	20.0 1.8

* Equivalent hydraulic diameter of rectangular channel 12.5 mm x 2.6 mm

Average deviation is defined as:

$$\delta_{avg} = \frac{1}{N}\sum_{N}^{1}\frac{(h_{predicted} - h_{measured})}{h_{measured}} \tag{13}$$

DISCUSSION

New Boundary for Regime III

The present research has provided Equation 10 as the boundary between Regime II and III. Figures 2 and 3 show test runs for which all data were predicted by Equation 10 to be in Regime III. It is seen that the agreement with the predictions of the present correlation is good. Without the boundary developed during the present research, all these data would have been grossly overpredicted as they would have been considered to be in Regime II.

The data analyzed in Shah (2009) were also examined to see the impact of the new boundary. Among the data of Akers et al. (1959) for propane, three were predicted to be in Regime III while they were in Regime II in the previous analysis. The mean deviation of these data was reduced from 43% to 23%. One data point of Akers et al. (1959) for R-12 was also found to be in Regime III; its deviation increased. None of the other data analyzed in Shah (2009) were found to be in Regime III.

Thus, overall the new boundary for Regime III was found to work reasonably well as deviations of most data were reduced by its introduction. It will be re-evaluated as more data become available.

New Fluids

Data for CO_2 and DME (dimethyl ether) were not analyzed in Shah (2009). Data for these fluids have been analyzed in the present study, as is discussed below.

As seen in Table 2, the data for DME cover a wide range of flow rates and show excellent agreement with the present correlation. Figure 4 shows comparison of some of these data with the present correlation.

As seen in Table 2, carbon dioxide data from four sources have been analyzed. All data show reasonable agreement except the data of Son and Oh (2012) at reduced pressure of 0.869 and 0.931, which are grossly overpredicted by the present correlation. Figure 5 compares their data at $p_r = 0.931$ with the present correlation as well as the correlation of Cavallini et al. (2006), which has been reported to agree with other data at very high reduced pressures. The data are seen to be much lower than the predictions of these correlations. Figure 6 shows a comparison with the data of Kondou and Hrnjak (2011) for carbon dioxide at p_r of 0.94. Excellent agreement with the present correlation is seen. Considering all the evidence, it appears that the high pressure data of Son and Oh (2012) are very unusual. In general, the present correlation can be considered reliable for CO_2. This is a significant result, as CO_2 is being used more and more because of its zero environmental impact.

Results Considering All Data

In Shah (2009), the new correlation was compared to 1189 data points from 39 studies with a mean deviation of 14.4%. These data included 22 fluids in horizontal, vertical

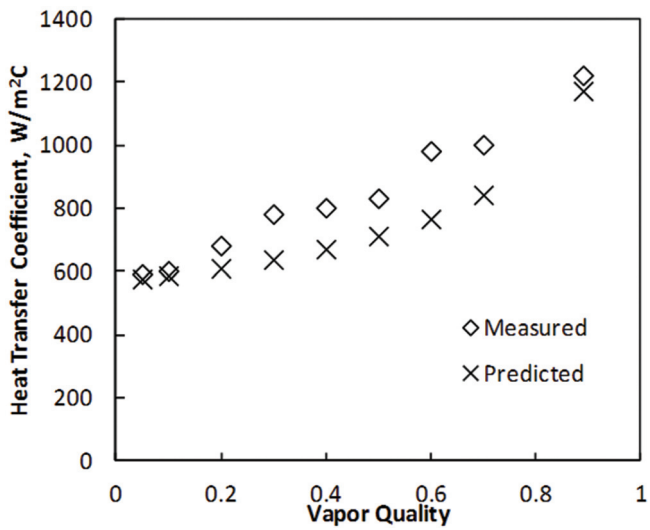

Figure 2 *Data of Son and Lee (2009) for R-22 compared with the present correlation. All data are in Regime III.* G = *52.5 kg/m²s (10.8 lb/ft²s),* D = *7.73 mm (0.3* in.*),* T_{SAT} = *40°C (104°F).*

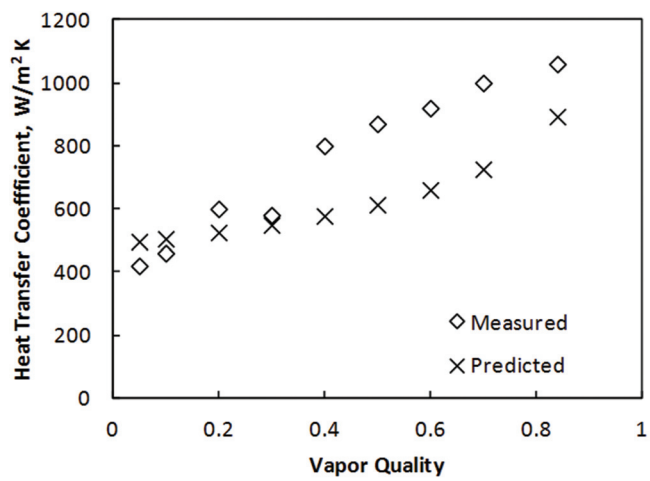

Figure 3 *Data of Son and Lee (2009) for R-134a compared with the present correlation. All data are in Regime III.* G = *52.5 kg/m²s (10.8 lb/ft²s),* D = *10.07 mm (0.4 in.),* T_{SAT} = *40°C (104°F).*

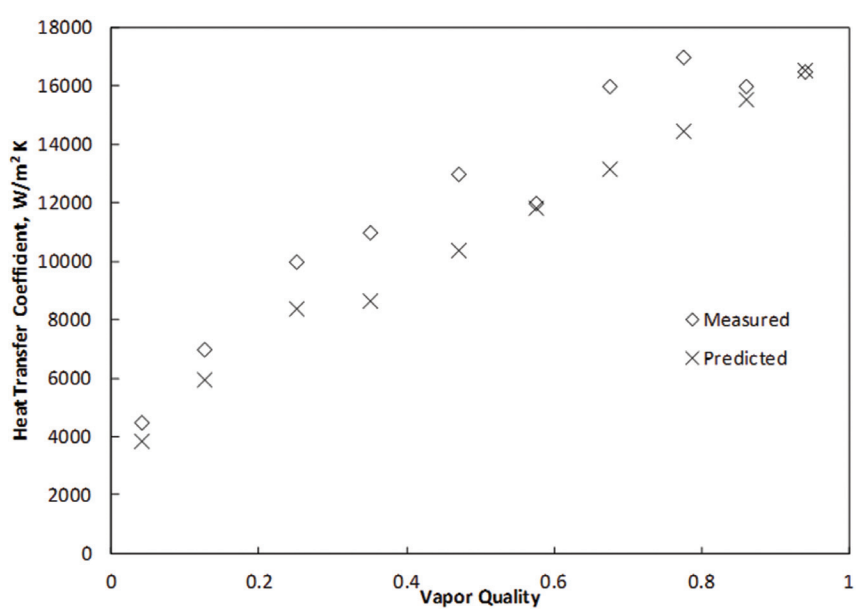

Figure 4 *Data of Afroz et al. (2008) for DME compared with the present correlation.* G = *500 kg/m²s (102.5 lb/ft²s)*

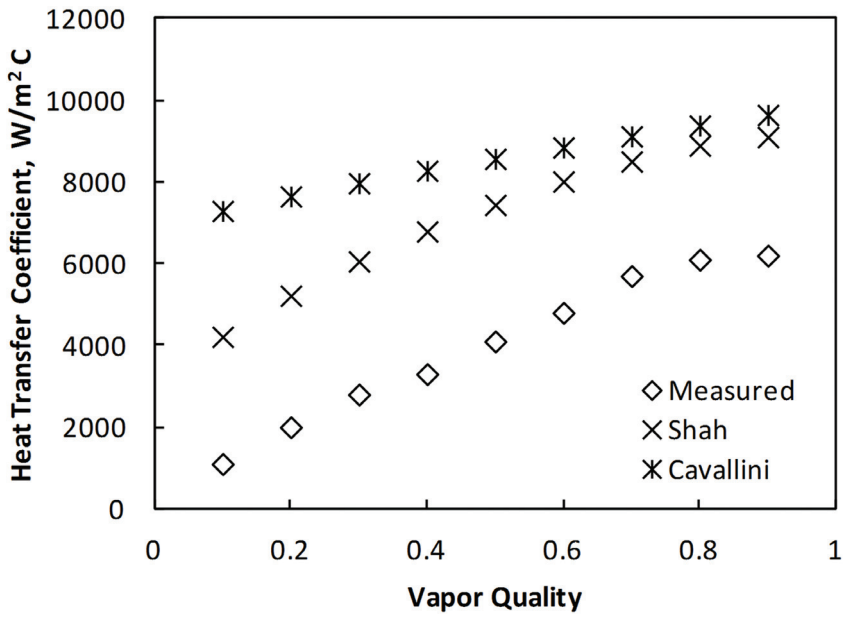

Figure 5 *Data of Son and Oh (2012) for CO_2 at* p_r *= 0.93,* G *= 800 kg/m^{2}s (164 lb/ft^{2}s) compared to the present correlation and the correlation of Cavallini et al. (2006).*

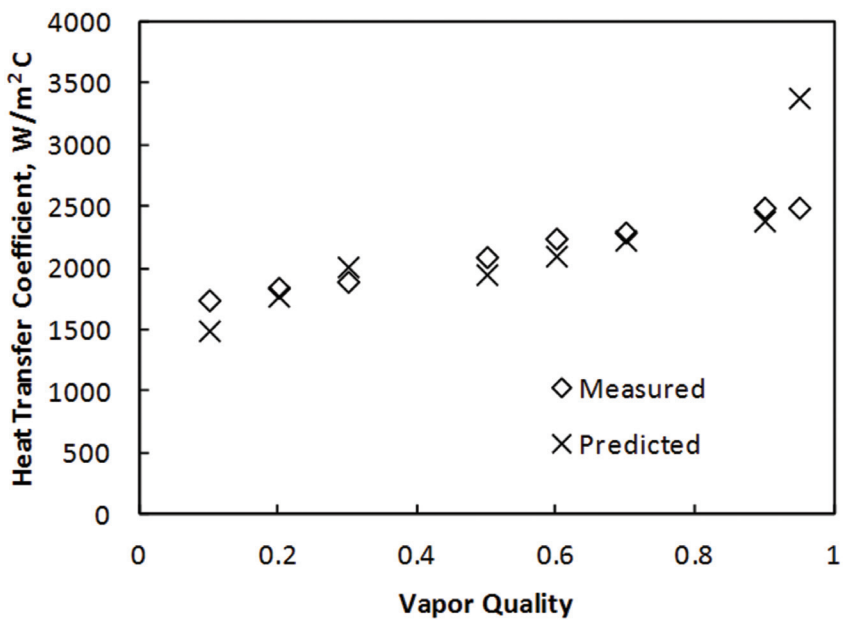

Figure 6 *Data of Kondou and Hrnjak (2011) for CO_2 compared to the present correlation.* p_r *= 0.9456,* G *= 150 kg/m^{2}s (30.8 lb/ft^{2}s).*

and inclined tubes. In the present study, 547 data points from 12 studies have been compared with the present correlation with a mean deviation of 20%. Thus, overall, 1736 data points for 24 fluids from 51 studies have been correlated with a mean deviation of 16.1%. The complete range of data is listed in Table 3.

Table 3. Complete Range of Parameters in the Data Showing Satisfactory Agreement with the Present Correlation

Parameter	
Fluids	Water, R-11, R-12, R-22, R-32, R-113, R-123, R-125, R-134a, R-142b, R-404A, R-410A, R-502, R-507, isobutane, propylene, propane, benzene, ethanol, methanol, toluene, Dowtherm 209, DME, CO_2
Tube diameter, mm (in.)	2 to 49 (0.079 to 1.93)
Tube orientations	Horizontal, vertical downwards, 15 degrees downwards
Reduced pressure	0.0008 to 0.946
G, kg/m^{2}s (lb/ft^{2}s)	4 to 820 (0.82 to 168.1)
Pr_f	1 to 18
Re_{LT}	68 to 84827
Re_{GT}	9534 to 523317
x	0.01 to 0.99
Z	0.005 to 20
Jg	0.06 to 20
Number of data points	1736
Number of data sources	51

CONCLUSION

1. The boundary between Regimes II and III for horizontal tubes in the author's correlation (Shah 2009) was undetermined and hence all data not in Regime I were considered to be in Regime II. This boundary has been determined in the present research. It has improved the accuracy of the correlation at low flow rates.
2. Comparison with the flow pattern map of El Hajal et al. (2003) showed that heat transfer Regime I corresponds to the mist, annular, and intermittent flow patterns of their map. Regimes II and III could not be clearly classified in terms of their flow regimes.
3. Data for two fluids not analyzed earlier, carbon dioxide and DME, were compared to the present correlation. All these data show adequate agreement with the present correlation, except for very high pressure data for CO_2 from one source. However, even higher pressure data from another source shows good agreement.
4. Considering all data analyzed earlier and in the present study, the present correlation has been compared to 1736 data points for 24 fluids from 51 sources with a mean deviation of 16.1%.
5. The results of the data analysis have been presented in the foregoing. The reader may draw his own conclusions regarding the applicability of this correlation. The author recommends it in the range of dimensional and dimensionless parameters covered by the data analyzed.

NOMENCLATURE

All equations are dimensionless. Any consistent system may be used.

D = inside diameter of tube
G = total mass flux (liquid + vapor)
g = acceleration due to gravity
h = heat transfer coefficient
h_I = heat transfer coefficient given by Equation 1
h_{LS} = heat transfer coefficient assuming liquid phase flowing alone in the tube
h_{LT} = heat transfer coefficient assuming all mass flowing as liquid
h_{Nu} = heat transfer coefficient given by Equation 2, the Nusselt equation
h_{TP} = two-phase heat transfer coefficient
J_g = dimensionless vapor velocity defined by Equation 8
k = thermal conductivity
N = number of data points
p_r = reduced pressure
Pr = Prandtl number
Re_{LS} = Reynolds number assuming liquid phase flowing alone, $= G(1 - x)D/\mu_f$
Re_{LT} = Reynolds number assuming total mass flowing as liquid, $= GD/\mu_f$
T_{SAT} = saturation temperature
x = vapor quality
Z = Shah's correlating parameter defined by Equation 9

Greek

μ = dynamic viscosity
ρ = density

Subscripts

f = of liquid
g = of vapor

REFERENCES

Afroz, H.M.M., A. Miyara, and K. Tsubaki 2008. Heat transfer coefficients and pressure drops during in-tube condensation of CO_2/DME mixture refrigerant. *International Journal of Refrigeration* 31:1458–66.

Akers, W.W., H.A. Deans, and O.K. Crosser. 1959. Condensing heat transfer within horizontal tubes. *Chemical Engineering Progress Symposium Series*, 59(29):171–6.

Breber, G., J.W. Palen, and J. Taborek. 1980. Prediction of horizontal tubeside condensation of pure components using flow regime criteria. *Journal of Heat Transfer* 102(3):471–6.

Cavallini, A., D.D. Col, L. Doretti, M. Matkovic, L. Rossetto, and C. Zilio. 2006. Condensation in horizontal smooth tubes: a new heat transfer model for heat exchanger design. *Heat Transfer Engineering* 27(8):31–8.

Dalkilic, A.S. and O. Agra. 2009. Experimental apparatus for the determination of condensation heat transfer coefficients for R-134a and R-600a flowing inside vertical and horizontal tubes respectively. *Proceedings of the 2009 ASME Summer Heat Transfer Conference* CA: San Francisco.

El Hajal, J., J. R. Thome, and A. Cavallini. 2003. Condensation in horizontal tubes, part I: two-phase flow pattern map. *International Journal of Heat and Mass Transfer* 46:3349–63.

Iqbal, O., and P. Bansal. 2012. In-tube condensation of CO_2 heat transfer in a horizontal smooth tube. *International Journal of Refrigeration* 35(2): 270–7.

Kondou, C., and P. Hrnjak. 2011. Heat rejection from R744 flow under uniform temperature cooling in a horizontal smooth tube around the critical point. *International Journal of Refrigeration* 34:719–31.

Lee, H., and C. Son. 2010. Condensation heat transfer and pressure drop characteristics of R-290, R-600a, R-134a, and R-22 in horizontal tubes. *Heat and Mass Transfer* 46:571–84.

Lemmon, E. W., M. L. Huber, M. O. McLinden. 2010. *NIST Reference Fluid Thermodynamic and Transport Properties*, REFPROP Version 9.0, NIST, Gaithersburg, MD.

McAdams, W.H. 1954. *Heat Transmission*, 3rd edition. New York: McGraw-Hill.

Shah, M.M. 1979. A general correlation for heat transfer during film condensation in pipes. *International Journal of Heat and Mass Transfer* 22:547–56.

Shah, M.M. 2009. An improved and extended general correlation for heat transfer during condensation in plain tubes. *HVAC&R Research* 15(5):889–913.

Shah, M.M. 2010. Heat Transfer during condensation inside small channels: applicability of general correlation for macrochannels. *Proceedings of the 14th International Heat Transfer Conference*. DC: Washington.

Son, C. and H. Lee. 2009. Condensation heat transfer characteristics of R-22, R-134a and R-410A in small diameter tubes. *Heat and Mass Transfer* 45:1153–66.

Son, C. and H. Oh. 2012. Condensation heat transfer characteristics of CO_2 in a horizontal smooth- and microfin-tube at high saturation temperatures. *Applied Thermal Engineering* 36:51–62.

Wen, M., C. Ho, and J. Hsieh. 2006. Condensation heat transfer and pressure drop characteristics of R-290 (propane), R-600 (butane), and a mixture of R-290/R-600 in the serpentine small-tube bank. *Applied Thermal Engineering*. 26:2045–53.

Zilly, J., J. Jang, and P. Hrnjak. 2003. Condensation of CO_2 at low temperature inside horizontal micro-finned tube. ACRC Report CR-49. University of Illinois at Urbana Champaign.

Wilson, M.J., T. A. Newell, J. C. Chato, and C.A. Infante Ferreira. 2003. Refrigerant charge, pressure drop, and condensation heat transfer in flattened tubes. *International Journal of Refrigeration* 26:443–51.